

# Why we must have Low-pT TOF for exclusive VM production?

Zhangbu Xu (BNL)

Thomas Ullrich

Daniel Brandenburg

Nicole Lewis

Zhenyu Ye (UIC)

# Motivation

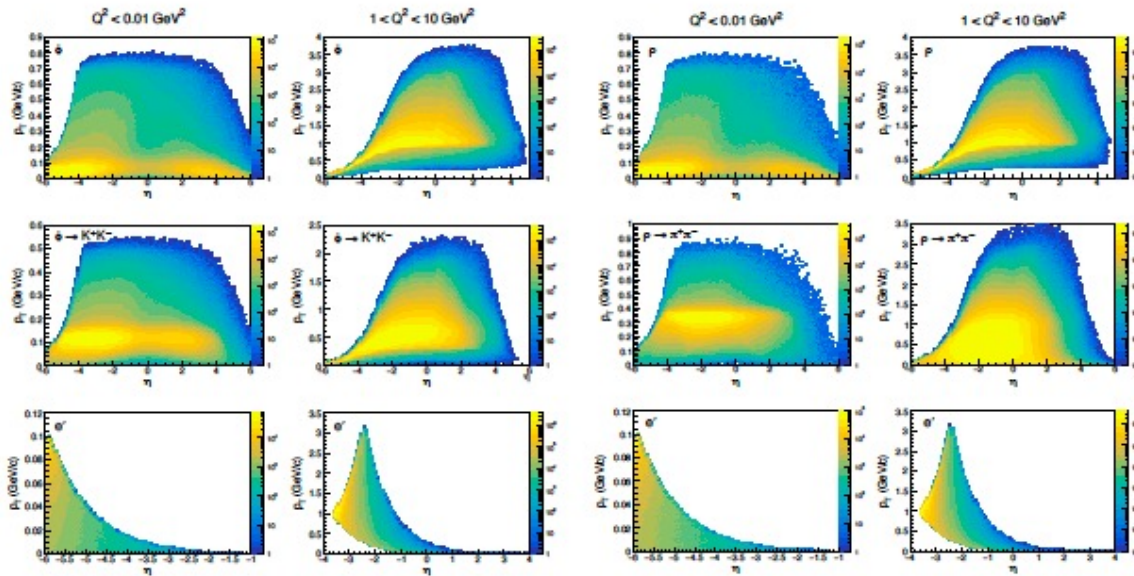


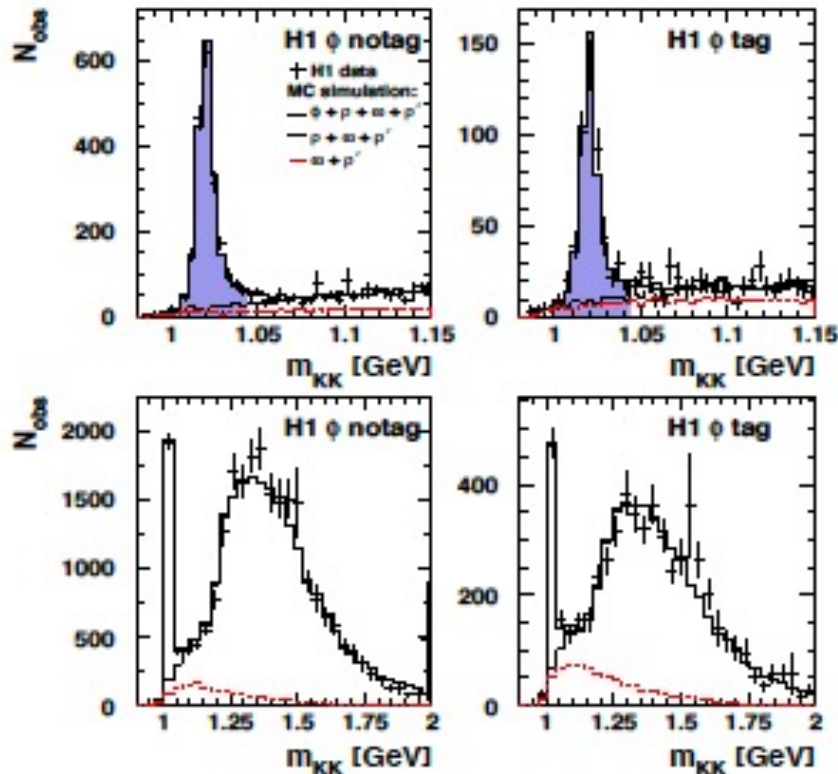
**Figure 8.84:** Left: Kinematics for diffractive  $e + Au \rightarrow e' + Au' + \phi$  with  $\phi$  decaying into  $K^+K^-$ . The left column is for photoproduction and the right for  $1 < Q^2 < 10 \text{ GeV}^2$ . Shown, from top to bottom are  $p_T$  versus pseudorapidity ( $\eta$ ) for  $\phi$ , kaons from the  $\phi$  decay, and the scattered electron. Right: Same for  $e + Au \rightarrow e' + Au' + \rho$  with  $\rho$  decaying into  $\pi^+\pi^-$ . Note the different scale on the vertical axis for photoproduction and electroproduction.

- a) Incoherent DVCS on deuteron+  $\pi^0$  + BH (central gamma or gamma gamma + p + n)
- b) Timelike Compton Scattering (central  $e^+e^-$ )
- c) Phi production in eA (central  $K^+K^-$  + intact/dissociated ion)
- d) Upsilon in ep ( $e^+e^-$  or  $\mu^+\mu^-$  + proton)
- e) Backward/u-channel photoproduction of omega ->  $\pi^0$  gamma.
- f)  $Z_c^+ \rightarrow J/\psi \pi^+$  (or other spectroscopy channel)

Exclusive and Tagging Group

Yellow Report

# Why do we need PID for exclusive?



If different VMs are all at different single fixed mass value, we do not have PID issue.

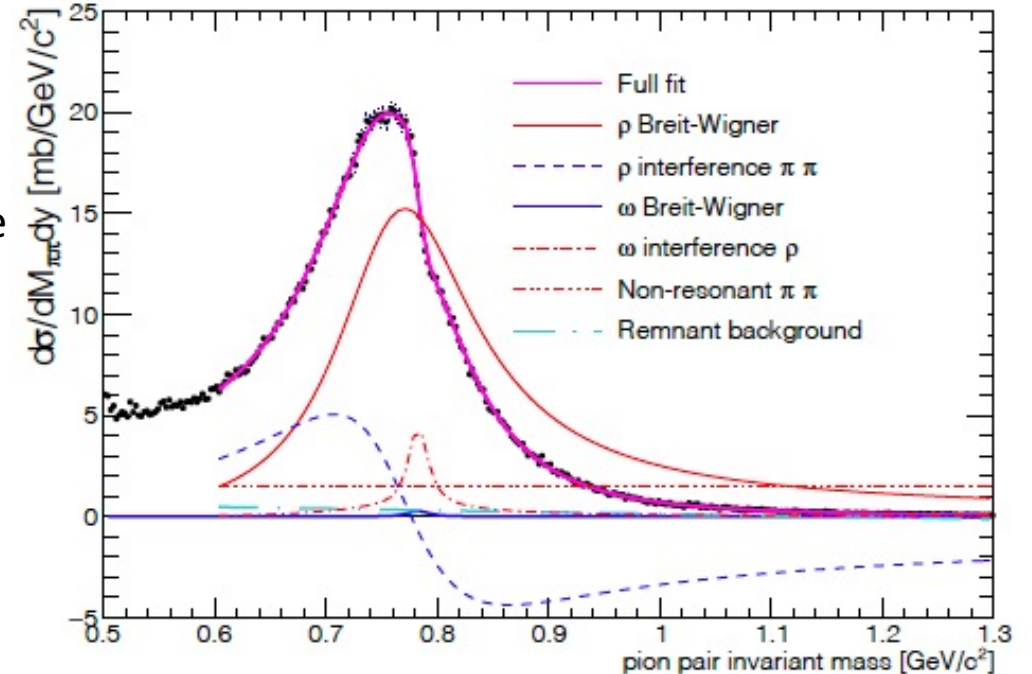
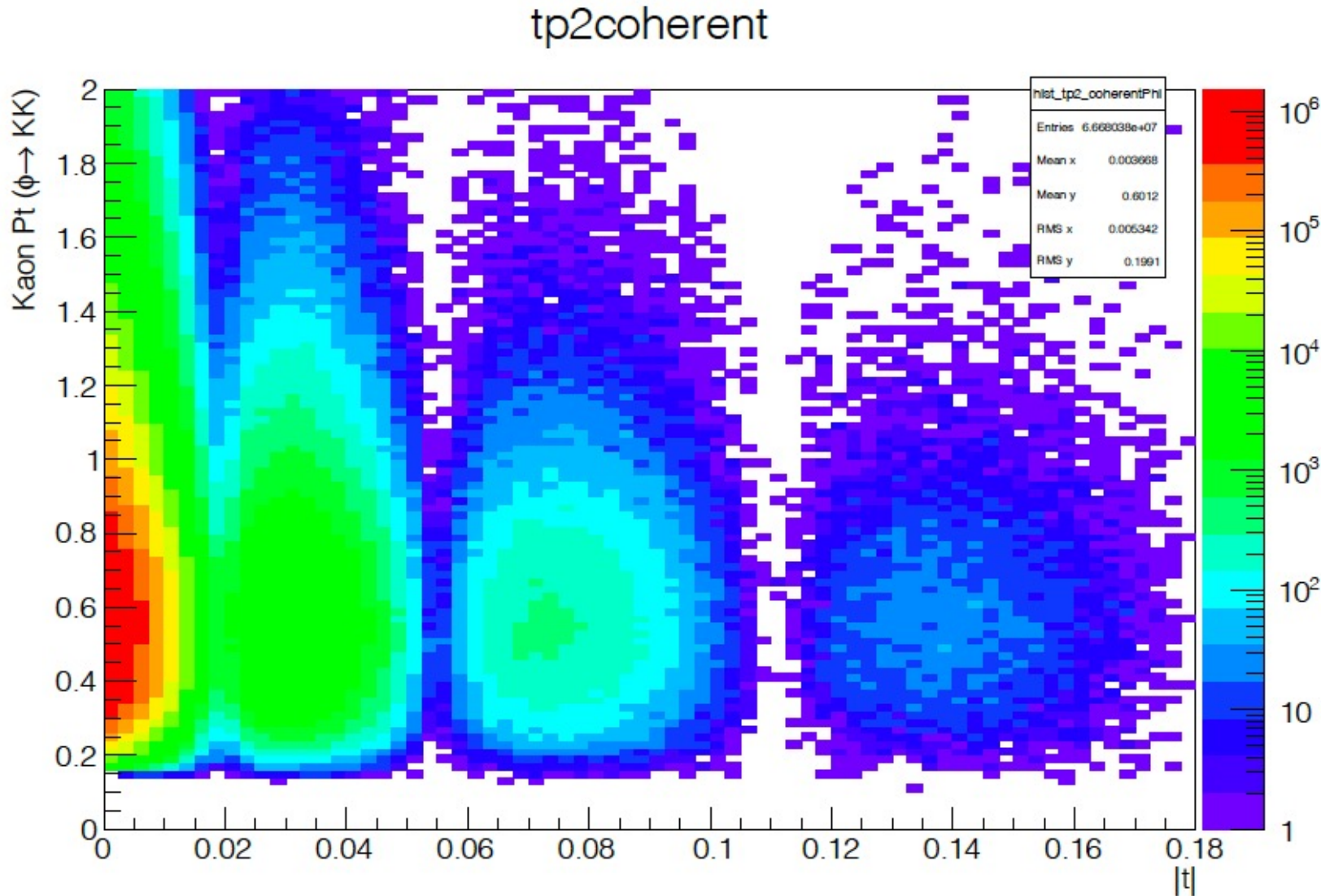


Figure 4: The  $\pi^+\pi^-$  invariant mass distribution for all selected  $\pi\pi$  candidates with  $p_T < 100$  MeV/c. The black markers show the data (in  $2.5$  MeV/ $c^2$  bins). The magenta curve is the modified Söding fit to the data in the range  $0.6 < M_{\pi\pi} < 1.3$  GeV/ $c^2$ . Also shown are the  $\rho^0$  Breit-Wigner component of the fit (brown curve), constant non-resonant pion pair component (brown-dashed curve), interference between non-resonant pion pairs and the  $\rho^0$  (blue-dashed curve), Breit-Wigner distribution for the  $\omega$  mesons (blue solid curve), interference between  $\rho^0$  and  $\omega$  (red-dashed curve), and a small contribution from the remnant background, fit by a linear polynomial (cyan-dashed curve).

Figure 6: Distributions of the invariant mass  $m_{KK}$ : (upper plots) in the  $\phi$  mass region, for the notag and tag samples separately; (lower plots) over an extended mass range, showing the  $\phi$  signal and the reflection of  $\rho$  production and the backgrounds. The dashed histograms show the sum of the  $\rho'$ ,  $\omega$  and  $\phi \rightarrow 3\pi$  backgrounds, the dotted histograms show in addition the  $\rho$  and non-resonant  $\pi\pi$  backgrounds, and the full histograms the  $\phi \rightarrow KK$  signal and the sum of all backgrounds. In (a) and (b), the mass domain where the cross section measurements are performed is shaded.

STAR, 1702.07705

# SARTRE simulation of $\phi \rightarrow KK$ kinematics



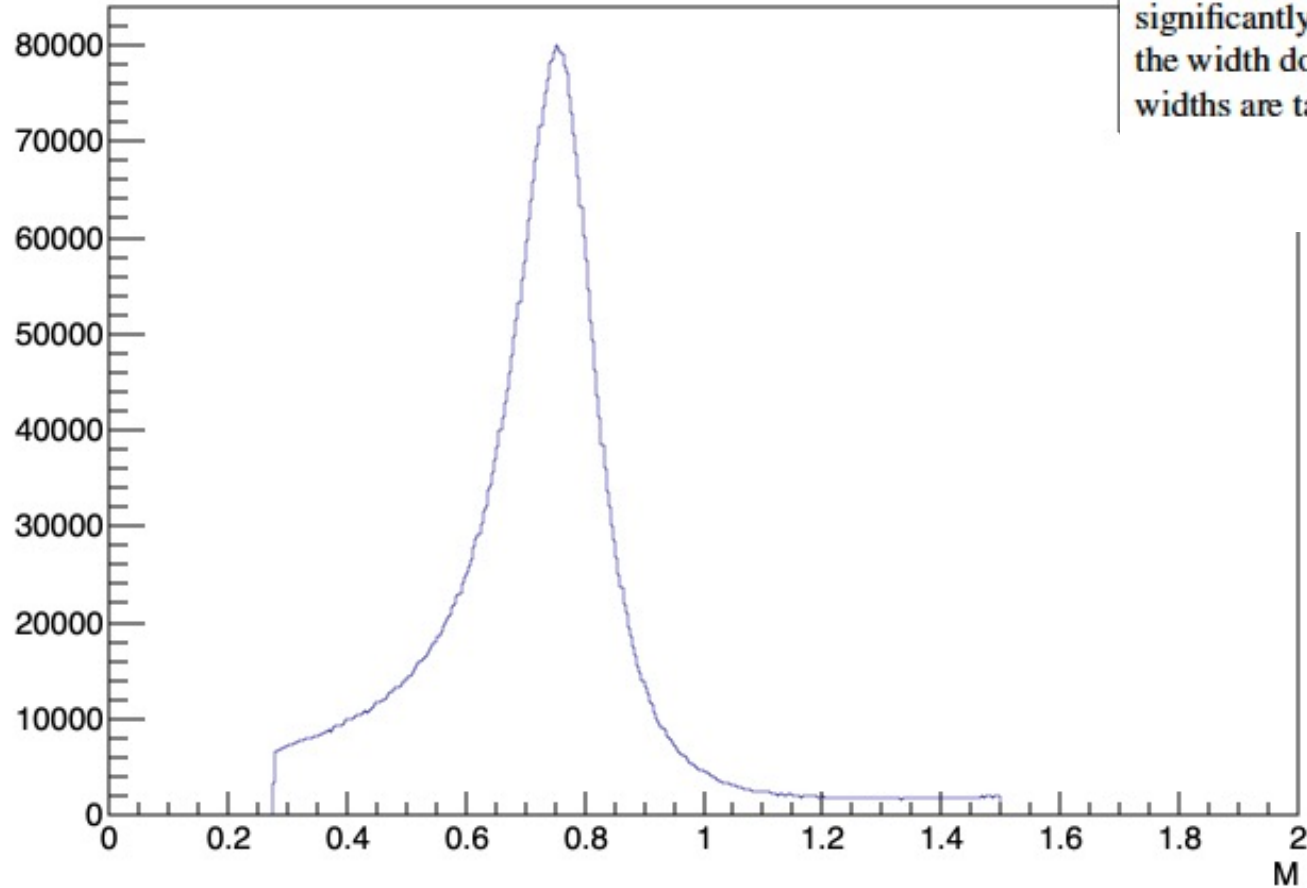
Exclusive  $\phi \rightarrow KK$   
In e+Au at 18+110 in SARTRE  
with  $|\eta| < 4$

Provided by Thomas  
in standard generator

Fixed mass value for all VM in SARTRE,  
Possible choices of implementing  
spectral functions:

1. Keep 3Vector p, change mass
2. Keep energy, change mass and 3Vector
3. Figure out how to implement energy and momentum conservation globally

# VM spectral function



$$\frac{d\sigma}{dM_{\pi^+\pi^-}} \propto \left| A_\rho \frac{\sqrt{M_{\pi\pi} M_\rho \Gamma_\rho}}{M_{\pi\pi}^2 - M_\rho^2 + i M_\rho \Gamma_\rho} + B_{\pi\pi} + C_\omega e^{i\phi_\omega} \frac{\sqrt{M_{\pi\pi} M_\omega \Gamma_{\omega \rightarrow \pi\pi}}}{M_{\pi\pi}^2 - M_\omega^2 + i M_\omega \Gamma_\omega} \right|^2 + f_p \quad (2)$$

where  $A_\rho$  is the  $\rho$  amplitude,  $B_{\pi\pi}$  is the amplitude for the direct pions,  $C_\omega$  is the amplitude for the  $\omega$ , and  $f_p$  is a linear polynomial that accounts for the remaining background. The momentum-dependent widths in Eqs. (3) and (4) below are motivated by the forms proposed in Ref. [29], where  $\Gamma_0$  is the pole width for each meson. Several variations of the dipion mass dependence for the  $\omega$  width were tried, but none were significantly different from a constant, reflecting the fact that the  $\omega$  width is small, and the width does not change significantly in that mass range. The momentum-dependent widths are taken to be

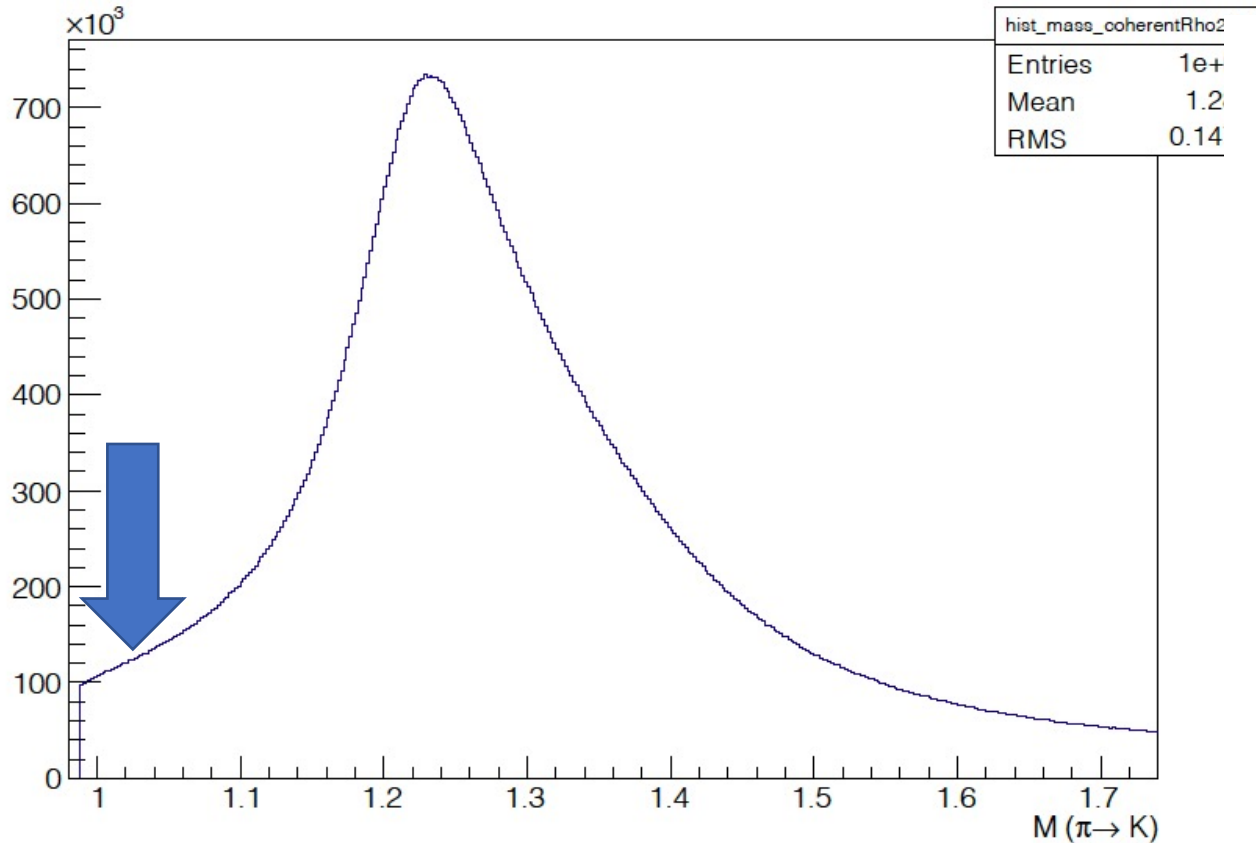
$$\Gamma_\rho = \Gamma_0 \frac{M_\rho}{M_{\pi\pi}} \left( \frac{M_{\pi\pi}^2 - 4m_\pi^2}{M_\rho^2 - 4m_\pi^2} \right)^{3/2} \quad (3)$$

Fit Parameter	value	units
$M_\rho$	$0.7762 \pm 0.0006$	GeV/c <sup>2</sup>
$\Gamma_\rho$	$0.156 \pm 0.001$	GeV/c <sup>2</sup>
$A_\rho$	$1.538 \pm 0.005$	
$B_{\pi\pi}$	$-1.21 \pm 0.01$	(GeV/c <sup>2</sup> ) <sup>-1/2</sup>
$C_\omega$	$0.55 \pm 0.04$	
$M_\omega$	$0.7824 \pm 0.0008$	GeV/c <sup>2</sup>
$\Gamma_\omega$	$0.017 \pm 0.002$	GeV/c <sup>2</sup>
$\phi_\omega$	$1.46 \pm 0.11$	radians
$f_p p_0$	$0.99 \pm 0.07$	(GeV/c <sup>2</sup> ) <sup>-1</sup>
$f_p p_1$	$-0.86 \pm 0.06$	(GeV/c <sup>2</sup> ) <sup>-2</sup>

Table 2: The results of fitting Eq. 2 to the data. The parameters  $p_0$  and  $p_1$  are for the polynomial background.

# Misidentified $\rho \rightarrow \pi\pi$ as $\phi \rightarrow KK$

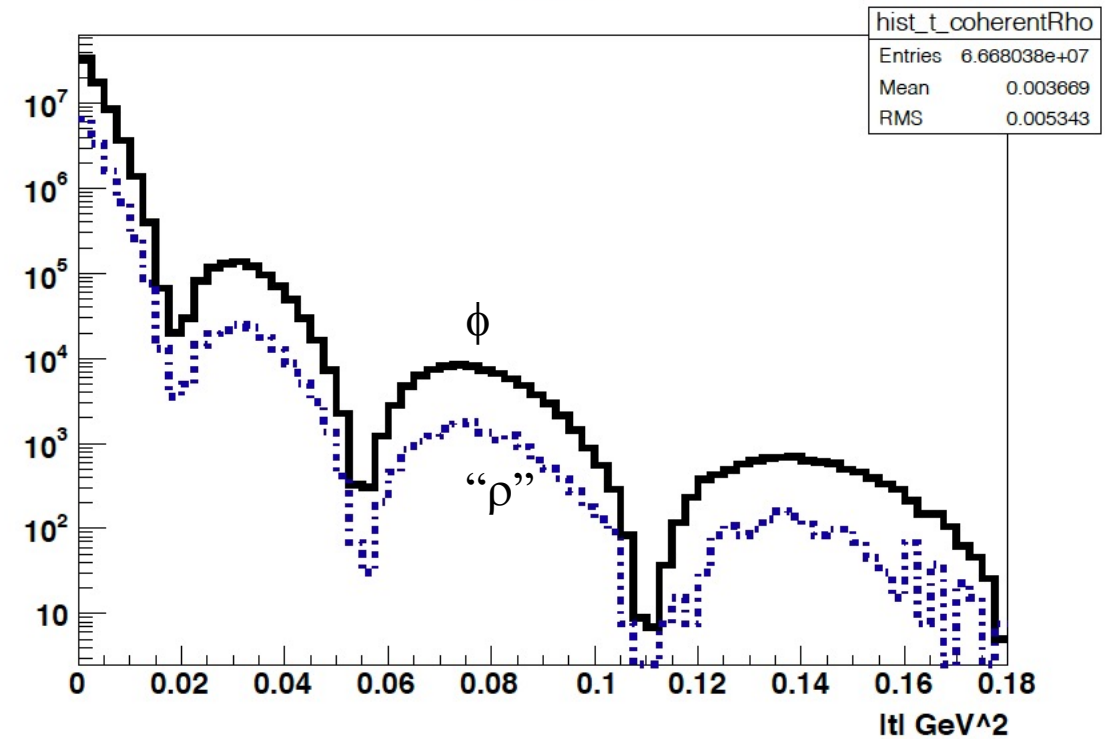
MassCoherent



Mass window  $\pm 20\text{MeV}$

Ignore other VM ( $\omega, \rho'$ ) contaminations for now

coherent

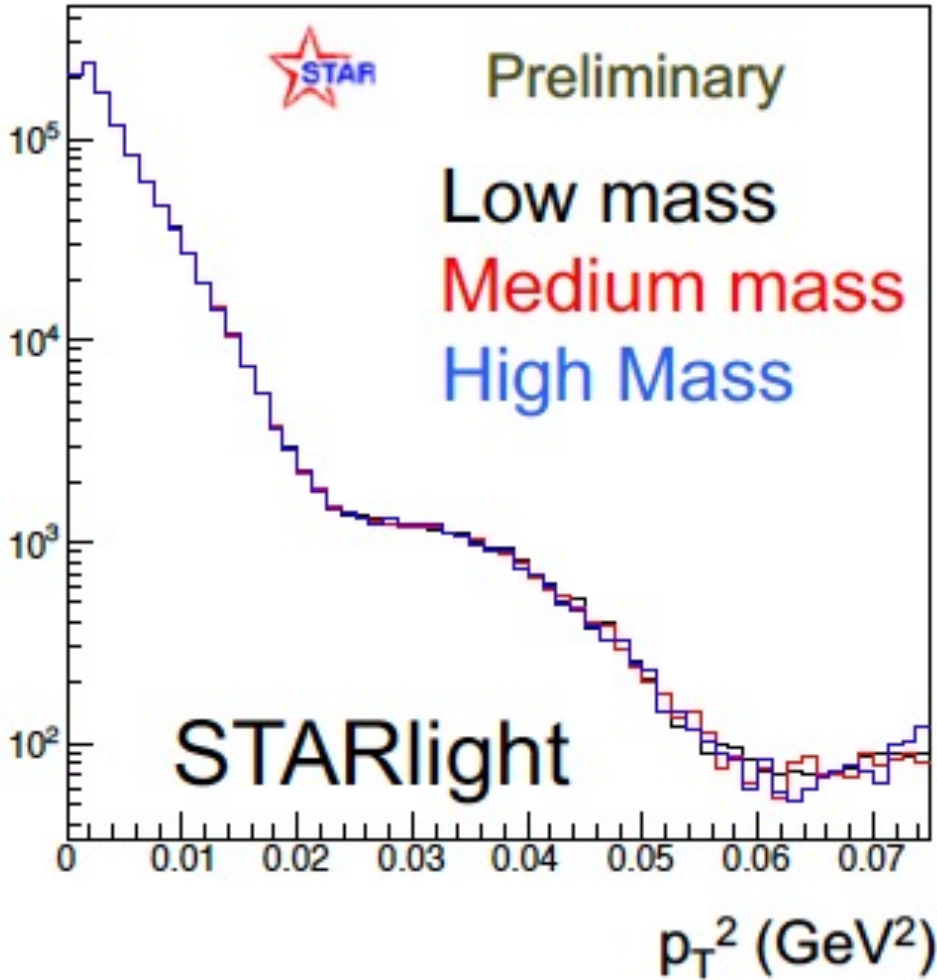
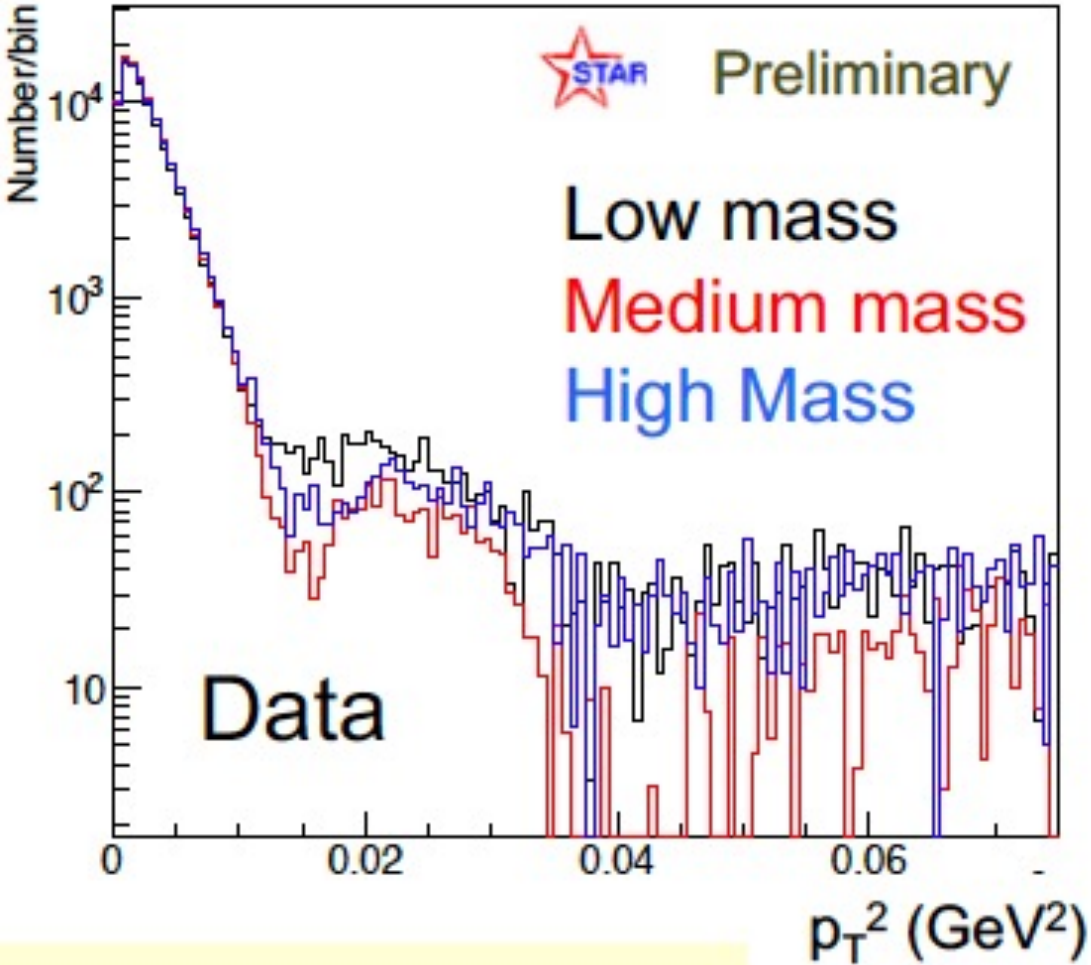


Rho/phi cross section is 7.6

15%, consistent with H1 result

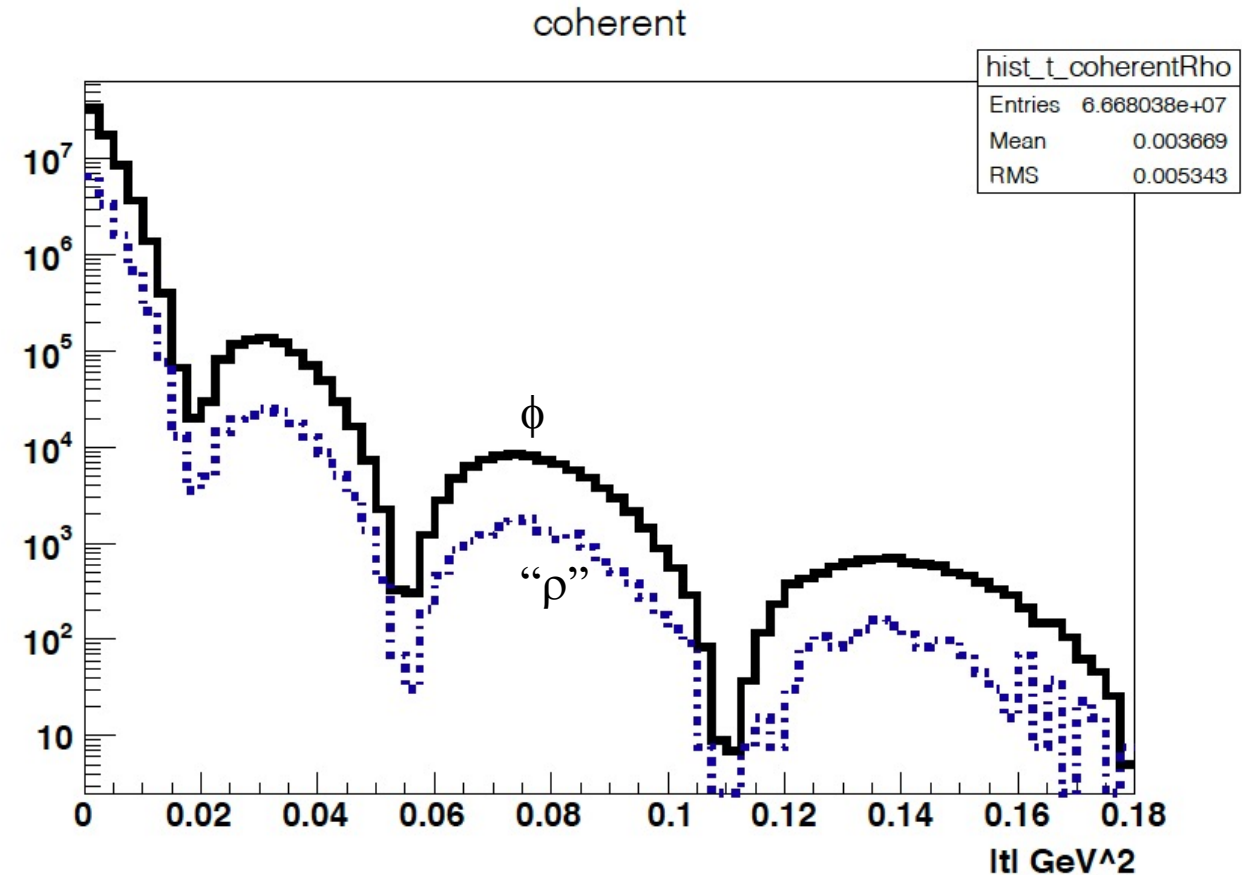
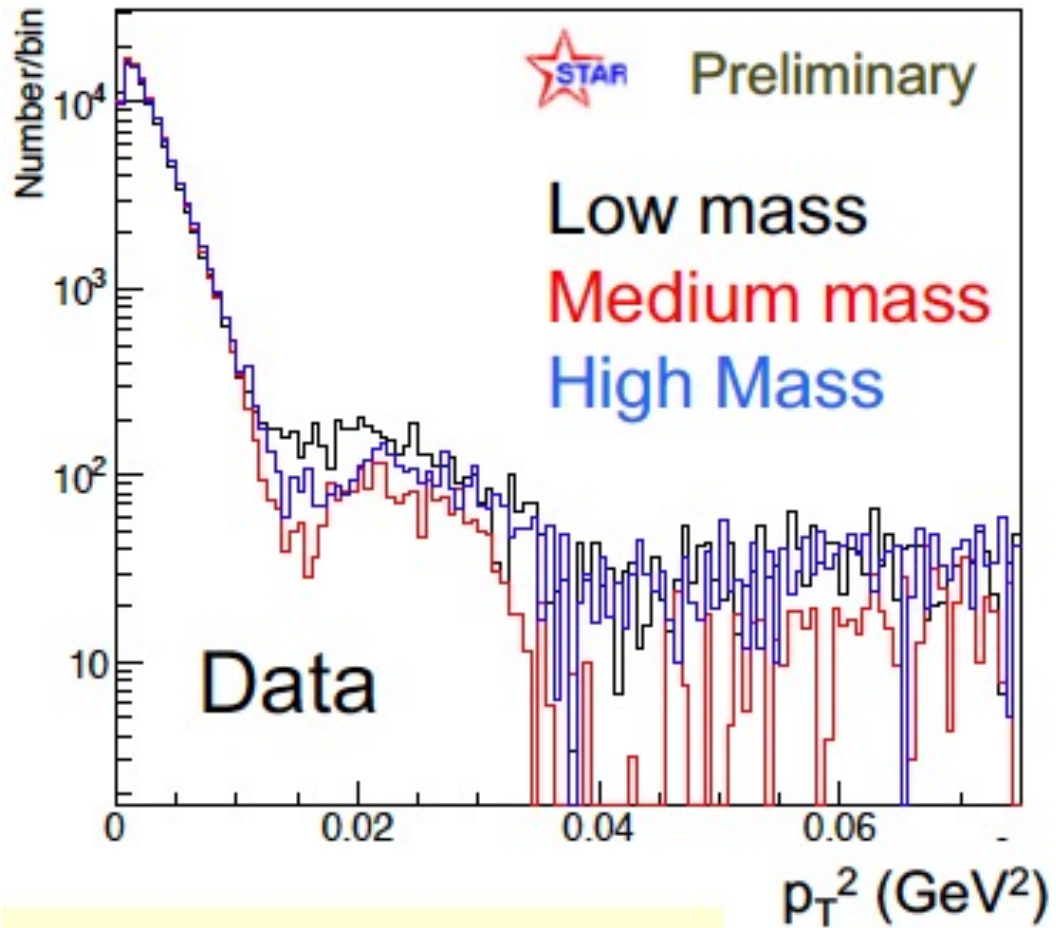
# Mass and Q2 evolution of diffractive pattern

Spencer Klein for STAR, DIS



If all mass and all particles of different kind would have had same diffractive pattern, we could just use rho.

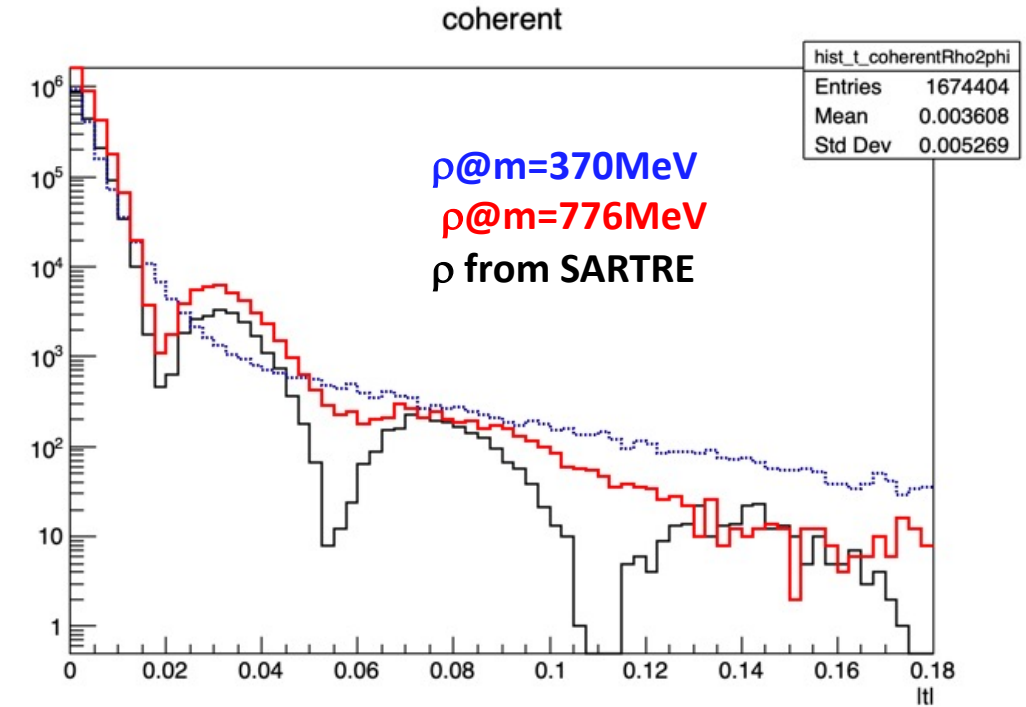
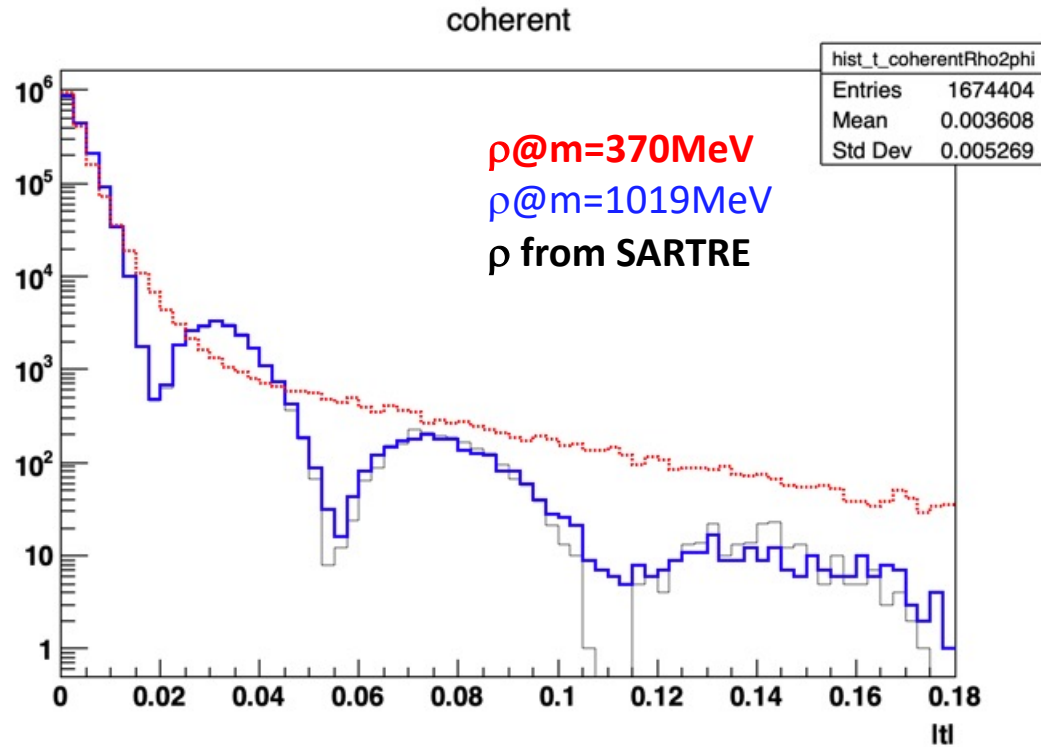
# Misidentified $\rho \rightarrow \pi\pi$ as $\phi \rightarrow KK$ could be worse



Rho and phi could smear and fill each other's diffractive patterns



# Naïve implementation of dipole smearing



VM wavefunction as a dipole  
probing nucleus

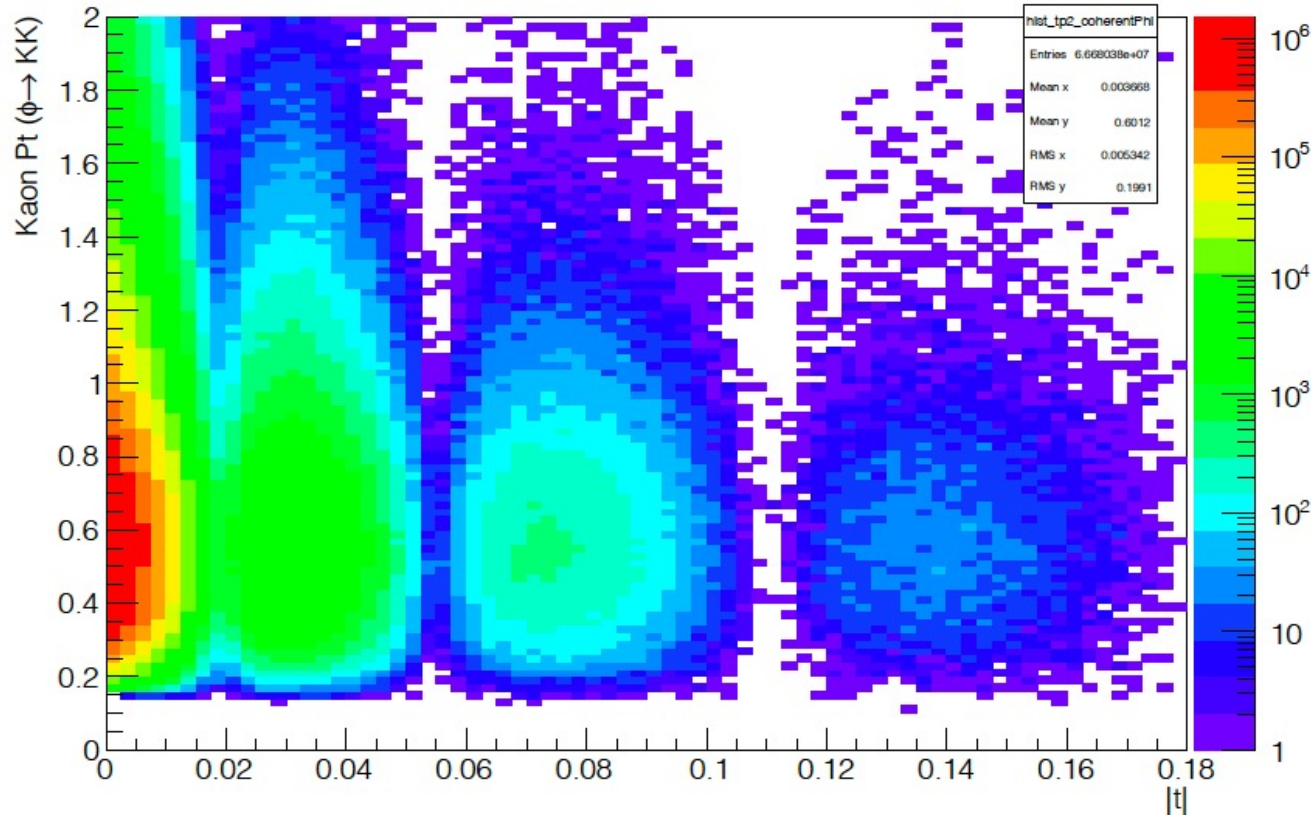
$$r \sim 1/m; \sigma_{r2}^2 = 1/m^4$$

$|t|$  smearing due to dipole size:  
convolution of  $|t|$  with a Gaussian  
smearing function:

$$\int f(t_0) e^{-\left(\frac{1}{t} - \frac{1}{t_0}\right)^2 / \left(\frac{2}{m^4}\right)}$$

# Pion/kaon PID

tp2coherent



RICH type of detector at 1m, if incident angle is  $>60^\circ$ , minimum pt reach the detector is  $0.9\text{GeV}/c$

dE/dx type of detector pion/kaon merge around  $p \sim 0.6\text{GeV}/c$

ACLGAD at  $\sim 0.5\text{m}$  with  $30\text{ps}$  resolution, **three particles in the event, eKK**, will have minimum pt reach of  $0.2\text{GeV}/c$  and pion/K separation at  $1.2\text{GeV}$  at  $3\sigma$ . Scale from the existing TOF performance at STAR

Allow reasonable overlap with other PID detectors and meet the YR science goal

# Chi2 method of TOF PID

$$\chi^2 = \frac{(dt_1 - a)^2}{\sigma_1^2} + \frac{(dt_2 - a)^2}{\sigma_2^2} + \frac{a^2}{\sigma_e^2}$$
$$= (dt_1^2/\sigma_1^2 + dt_2^2/\sigma_2^2) - (dt_1/\sigma_1^2 + dt_2/\sigma_2^2)^2 \sigma^2$$

$$dt = t_{\text{TOF}} - L/\beta_k, \quad \sigma_1 = \sigma_2 = 25 \text{ ps}, \quad \sigma_e = 30 \text{ ps}$$

$$a = (dt_1/\sigma_1^2 + dt_2/\sigma_2^2) \sigma^2$$

$$1/\sigma^2 = 1/\sigma_1^2 + 1/\sigma_2^2 + 1/\sigma_e^2$$

pathlength  $L = 2p/(30B) \text{Asin}(30B * R/2/p_t)$

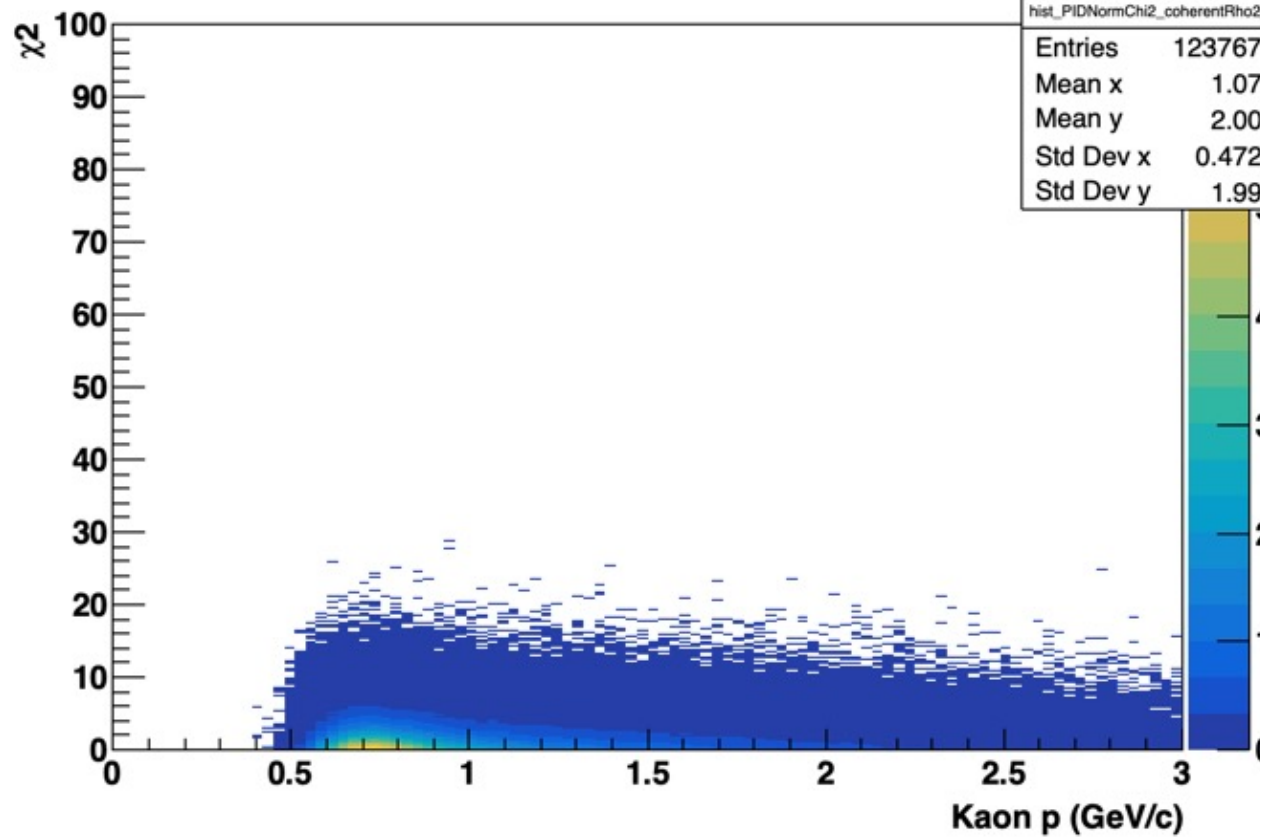
$R = 50 \text{ cm}$ : radial location of LGAD TOF

$B = 3 \text{ T}$  Bfield

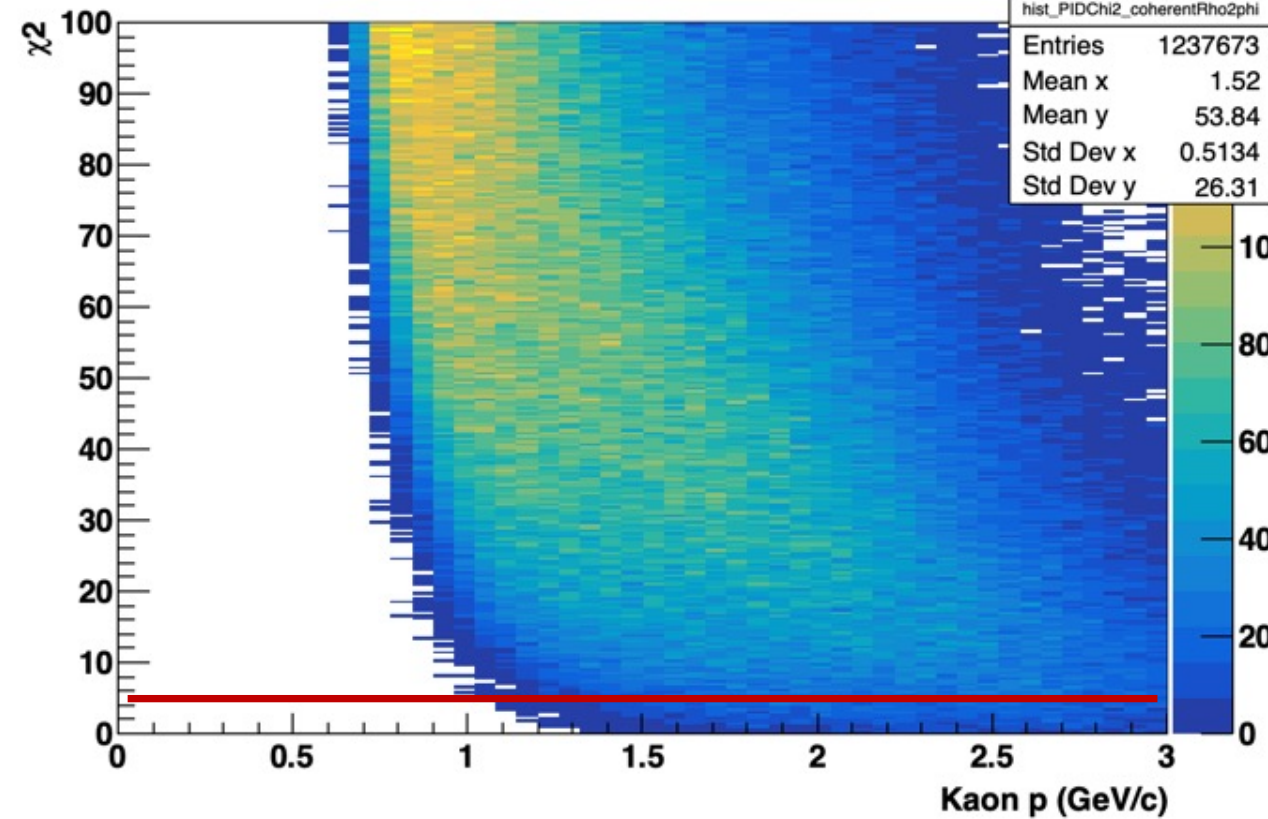
$p, p_t$ : momentum of daughters (GeV/c)

# Kaon vs pion pairs

PIDNormChi2coherent



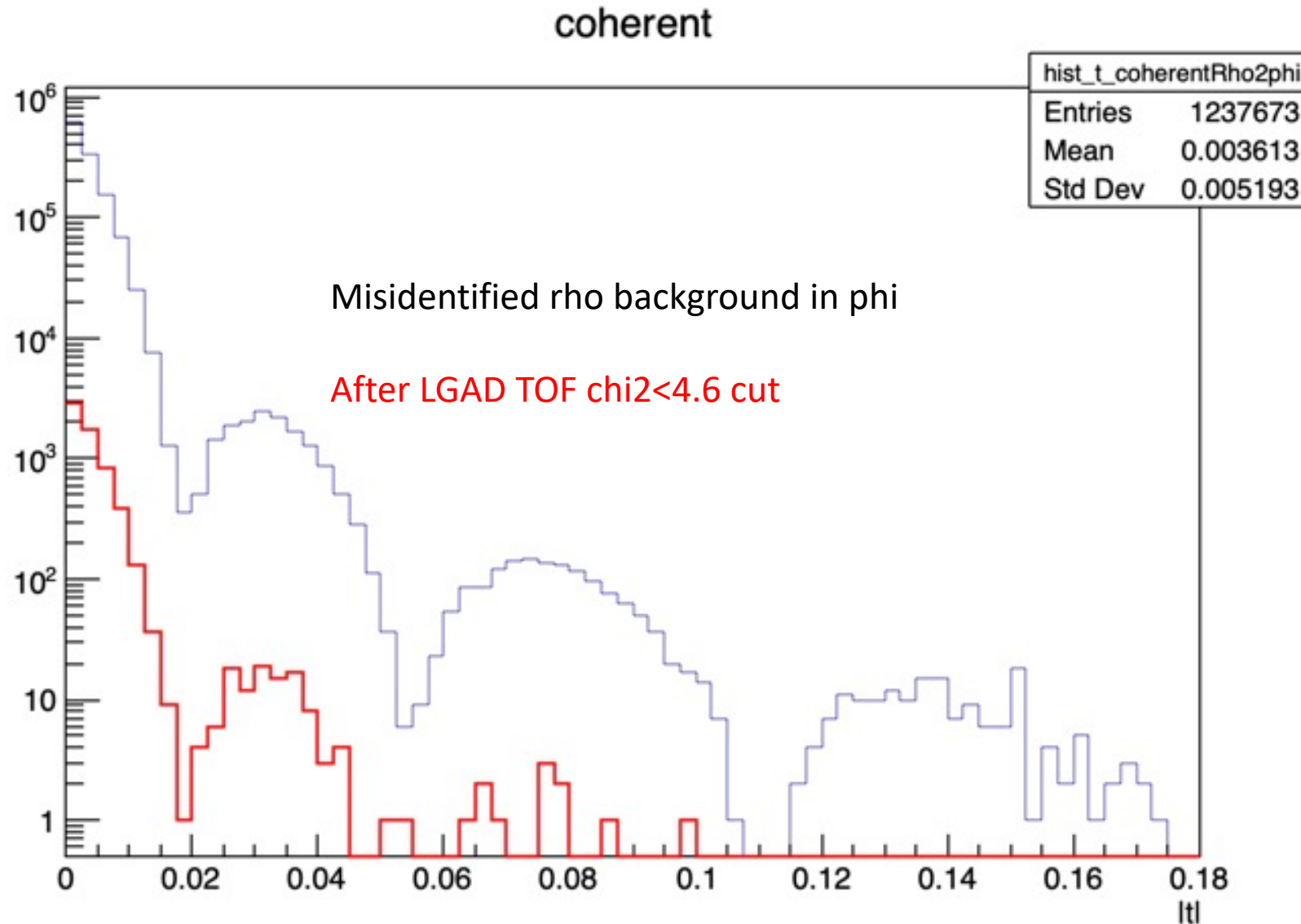
PIDChi2coherent



Effective even at  $p \sim 3 \text{ GeV}/c$

$\text{Chi}^2 < 4.6$  (90% efficiency) for correct pairs

# Background rejection power



>100 rejection power  
LGAD TOF ALONE

# Summary

- A low-pT TOF is required for achieving YR science goals on exclusive VM diffractive measurement
- ACLGAD right outside of silicon tracker will meet the requirement
- More details and realistic simulations are necessary for the proposal but all the simulation and assessments are based on the existing data and simulations

# Different pseudorapidity range $\pm 2$ vs $\pm 4$

